Journal Pre-proof

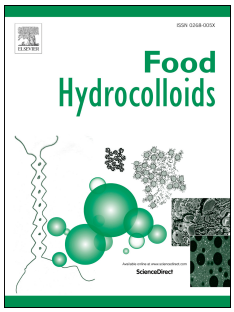

Improving the *in vitro* digestibility of rice starch by thermomechanically assisted complexation with guar gum

Hai He, Chengdeng Chi, Fengwei Xie, Xiaoxi Li, Yi Liang, Ling Chen

PII: S0268-005X(19)32397-5

DOI: https://doi.org/10.1016/j.foodhyd.2019.105637

Reference: FOOHYD 105637

To appear in: *Food Hydrocolloids*

Received Date: 12 October 2019

Revised Date: 12 December 2019

Accepted Date: 30 December 2019

Please cite this article as: He, H., Chi, C., Xie, F., Li, X., Liang, Y., Chen, L., Improving the *in vitro* digestibility of rice starch by thermomechanically assisted complexation with guar gum, *Food Hydrocolloids* (2020), doi: https://doi.org/10.1016/j.foodhyd.2019.105637.

CRediT author statement:

Hai He: Methodology, Validation, Formal analysis, Investigation, Data Curation, Writing - Original Draft, Visualization. **Chengdeng Chi:** Writing - Review & Editing. **Fengwei Xie:** Methodology, Resources, Writing - Review & Editing, Visualization, Supervision, Funding acquisition. **Xiaoxi Li:** Conceptualization, Methodology, Writing - Review & Editing, Resources. **Yi Liang:** Resources. **Ling Chen:** Conceptualization, Methodology, Resources, Supervision, Project administration, Funding acquisition.

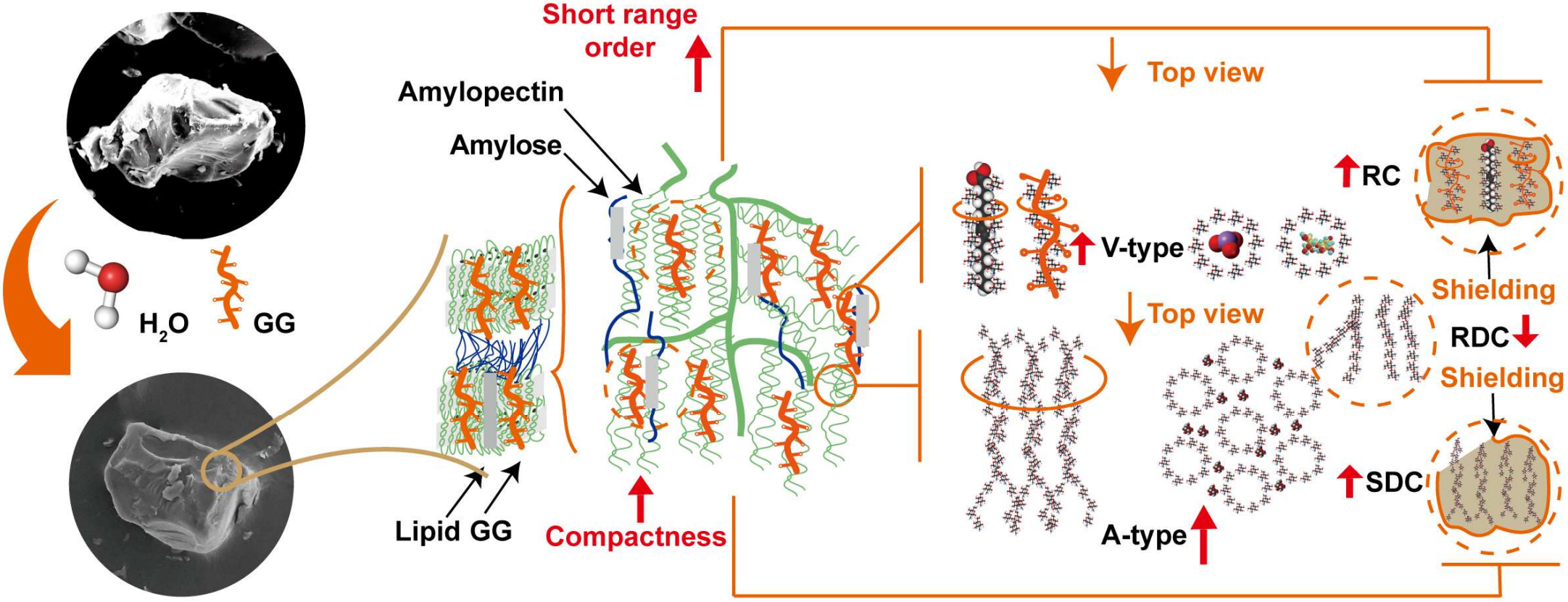
Short range order
Amylopectin
Amylose
Lipid GG
Compactness
Top view
V-type
Top view
A-type
RC
Shielding
RDC
Shielding
SDC
H2O
GG

Improving the *in vitro* digestibility of rice starch by thermomechanically assisted complexation with guar gum

Hai He [a], Chengdeng Chi [a], Fengwei Xie [b, c,†], Xiaoxi Li [a], Yi Liang [d], Ling Chen [a,*]

[a] Ministry of Education Engineering Research Center of Starch & Protein Processing, Guangdong Province Key Laboratory for Green Processing of Natural Products and Product Safety, School of Food Science and Engineering, South China University of Technology, Guangzhou, Guangdong, 510640, China.

[b] International Institute for Nanocomposites Manufacturing (IINM), WMG, University of Warwick, Coventry CV4 7AL, United Kingdom.

[c] School of Chemical Engineering, The University of Queensland, Brisbane, Qld 4072, Australia.

[d] Guangdong Zhongqing Font Biochemical Science and Technology Co., Ltd., Maoming, Guangdong 525427, China.

*Corresponding author. E-mail address: felchen@scut.edu.cn (L. Chen)

†Corresponding author. E-mail address: d.xie.2@warwick.ac.uk, f.xie@uq.edu.au (F. Xie)

ABSTRACT

The effects of thermomechanical treatment and guar gum (GG) addition on the *in vitro* digestibility of rice starch have been investigated. Rice starch added with GG at concentrations of 0, 0.025, 0.05, 0.075, or 0.10 g/100 g (wet basis) was subject to a micro-extrusion process. The *in vitro* digestibility, predicted glycemic index (pGI), and multi-scale structures (granule, lamellar, crystalline, and molecular structures) were examined. Micro-extruded rice starch (MERS) with GG presented reduced digestion rate and pGI, a higher degree of structural ordering, and altered crystalline, single-helical and double-helical structures. Using Pearson correlation analysis, the relationships among extrusion, the molecular interaction and multi-scale structure, and the digestibility were established. The content of resistant components (RC) was positively correlated with crystallinity (r = 0.836, $p < 0.05$), fractal dimension (r = 0.966, $p < 0.05$), A-type crystallinity (r = 0.954, $p < 0.01$), V-type crystallinity (r = 0.987, $p < 0.05$), $R_{1047/1022}$ (r = 0.987, $p < 0.05$), single-helix content (r = 0.897, $p < 0.05$), and double-helix content (r = 0.991, $p < 0.01$); and was negatively correlated with pGI (r = −0.947, $p < 0.05$). Overall, this study showed that thermomechanical treatment assisted the complexation of GG with starch, which could be an effective means to improve the resistant properties of rice starch.

Keywords: Rice starch; Extrusion; Guar gum; Molecular interaction; Digestive properties

1 Introduction

With the social development and the evolution of the human diet and disease spectrum, there has been an increasing focus on dietary nutrition and health (Crawford et al., 2014; Fang, Li, & Liu, 2016). Rice is the main source of carbohydrate for people, especially in Asia. It can be easily digested in the human digestive tract, providing the body with energy to prevent the occurrence of symptoms such as hunger and fatigue (Guerrant, Dutcher, & Brown, 1937). However, rice has a high glycemic index (GI), resulting in a high blood glucose response level after consumption, which leads to unstable blood sugar levels. This can cause insulin resistance and induce type II diabetes mellitus and related complications, thus, worsening human health (Miller, Pang, & Bramall, 1992; Roberts, 2000). Starch is an important component of rice, accounting for more than 80% of the total composition of rice. It is crucial to develop rice products with lower postprandial blood glucose response levels (Thompson, Winham, & Hutchins, 2012). Therefore, improving the resistant properties of rice starch, suppressing the postprandial blood glucose response to rice, and regulating the nutritional value of rice products are essential for developing rice-containing healthy foods and adjusting consumers' dietary structure.

Guar gum (GG) is another important food component. The molecular structure of GG consists of a D-mannose unit connected by a β-1,4-glycosidic bond to form its main chain, with D-galactose as side chains connected to the main chain by α-1,6 glycoside bond. It has a galactose/mannose ratio of approximately 1:2, with an average relative molecular mass of 200,000–300,000 (Mudgil, Barak, & Khatkar, 2014). GG can affect the functionality and nutritional characteristics of starch-based food products by non-covalent actions. Moreover, GG can be used as a dietary fiber to promote human

health (Chung, Liu, & Lim, 2007). As a dietary supplement, GG swells and then intertwines with other food components to form a network structure. This slows down the process of gastric emptying and subsides hunger and eating desire, which is particularly suitable for those who are obese or on diet (Butt, Shahzadi, Sharif, & Nasir, 2007). In the human colon, GG can be fermented by resident bacteria, producing short-chain fatty acids that protect the digestive tract and prevent bowel cancer (Shahzadi, Butt, Sharif, & Nasir, 2007). Bordoloi et al. (Bordoloi, Singh, & Kaur, 2012) reported that when potato starch was added with pectin, cellulose or GG, the digestion rate of the starch was significantly reduced owing to the physical embedding of GG. Jang et al. (Jang, Bae, & Lee, 2015) suggested that GG could induce the structural recombination of starch and significantly reduce the sugar index of noodles made from wheat flour or whole wheat flour.

The extrusion of starch can be considered as a ‘green’ processing technology where starch is plasticized with water under high temperature, shear, and pressure. During the extrusion process, starch is re-linked with a strengthened intermolecular hydrogen-bonded network, finally resulting in kinetic and thermodynamic stabilities (Gomez & Aguilera, 2010). Extrusion can modify the starch granule morphology, semicrystalline lamellar thickness, crystalline structure, molecular mass and its distribution, and linear/branched-chain starch contents (Lai & Kokini, 1991; Ye, Hu, Luo, Wei, & Liu, 2017). Besides, starch chain aggregates on different scales can be formed and the starch digestibility can be regulated (Fan et al., 2018).

The combination of extrusion treatment and GG addition is likely to produce rice starch with increased enzymatic resistance, which is conducive to human health. However, limited research can be found regarding the effect of extrusion on the GG complexation with starch. GG molecules may

induce chain rearrangement and aggregation through non-covalent interactions, such as hydrogen bonding and van der Waals forces, thus, changing the susceptibility of starch molecules to enzymes (Zheng et al., 2019). This current study aimed at understanding the combined effects of GG addition and extrusion treatment, for which the digestibility of micro-extruded rice starch (MERS) complexed with GG was analyzed using scanning electron microscopy (SEM), Fourier-transform infrared spectroscopy (FTIR), X-ray diffraction (XRD), small-angle X-ray scattering (SAXS), and ^{13}C nuclear magnetic resonance (NMR). Based on these analyses, we explored how the altered multi-scale structure of rice starch influence its digestibility. A relevant model was established and the mechanism for these effects was elucidated.

2 Materials and methods

2.1 Materials

Rice starch (GABIOSTA-F) was supplied by Jiangxi Jinnong Biotechnology Co., Ltd. (Wuxi, China), which contains 11.55% (d.b) moisture, 0.20% (d.b) lipid, 0.65% (d.b) protein, and 0.38% (d.b) ash. Food-grade guar gum (GG) was provided by Guangzhou Feibo Biotechnology Co., Ltd. (China). Pancreatic α-amylase (A3306) was purchased from Sigma (USA). A glucose oxidation kit (GOPOD) was bought from Megazyme (Ireland). All other chemical reagents used in this study were of analytical grade.

2.2 Preparation of micro-extruded rice starch (MERS) with guar gum (GG)

Rice starch (20 g, dry weight) was mixed with GG (2.5%, 5%, 7.5%, 10%, w/w, based on rice starch) in a flask. The mixture of rice starch and GG was adjusted to 40% moisture content, which

was then extruded in a Haake MiniLab II micro-compounder (Thermo Fisher Scientific, USA) at 150 rpm and 85 °C. The material was directly extruded without circulation in the micro-compounder. The residence time was about 5 min. The extrudates were dried at 40 °C for 24 h, and ground with a laboratory-scale grinder to pass through a 100-mesh sieve. According to the different amounts of GG added, micro-extruded rice starch (MERS) samples with GG were named in the form of "MERS/GG-X", in which "GG" represented guar gum, and "X" represented the content of added GG (%). The MERS sample without GG was named MERS/GG-0. These samples were compared with native rice starch (NRS).

2.3 *In vitro* starch digestibility

In vitro digestibility was measured based on the Englyst method (Englyst & Cummings, 1985) with slight modifications (Wang, Wang, Li, Chen, & Zhang, 2017). Considering the chemical structure of GG, non-digestive components may include not only resistant starch but also GG. Therefore, the digestive properties of MERS samples with GG were measured by the proportions of rapidly digestible components (RDC), which were hydrolyzed by incubation within 20 min, of resistant components (RC), which were remain unhydrolyzed after 120 min of incubation, and of slowly digestible components (SDC), which were calculated as the difference between RDC and RC.

2.4 Predicted glycemic index (pGI)

The hydrolysis index (HI) was calculated on the basis of the starch hydrolysis curve (0–180 min) as the percentage of total glucose released over 180 min in comparison with that released from white bread over the same duration (Goñi, Garciaalonso, & Sauracalixto, 1997; Jenkins et al., 1981). The

glycemic index (GI) was then estimated by using the equation used by Goni et al. (Goñi et al., 1997) with slight modifications (GI = 44.78 + 0.3797 × HI).

2.5 First-order kinetic analysis of *in vitro* digestibility

The logarithm of the slope (LoS) graphical method was used to study the *in vitro* digestibility of MERS samples and to predict their physiological response (Butterworth, Frederick, Terri, Hamung, & Peter, 2012; Dhital, Warren, Butterworth, Ellis, & Gidley, 2017; Xu, Kuang, Wang, Zhou, & Wang, 2017). The digestibility was fitted to the first-order kinetic as shown in Eq. (1):

$$C_t = C_\infty \left(1 - e^{-kt}\right) \quad (1)$$

where C_t is the digested components ratio of the samples, C_∞ is the digested components ratio at the end of the reaction, and k is the first-order rate constant.

By expressing the first derivative of the first-order equation in a logarithmic form, we obtained a logarithmic slope (LoS) plot:

$$ln(\frac{dC}{dt}) = -kt + ln(C_\infty k) \quad (2)$$

where $ln(dC/dt)$ represents the logarithm of the slope, k and C_∞ were used to construct a model-fitted starch digestion curve according to Eq. (1).

2.6 GPC-MALS analysis

The weight-average molecular mass (M_w), mean square radius of gyration, and molecular mass (M) distribution of the samples were analysed using a gel permeation chromatography (GPC) system coupled with a multi-angle light scattering detector and a refractive index (RI) detector, as described in our previous studies (Liu, Chen, Xu, Liang, & Zheng, 2019).

2.7 Determination of amylose content

The amylose content of starch was determined using the iodine reagent method (Lim et al., 2015). 100 mg of starch was accurately weighed and dispersed in a 1M NaOH solution, which was then diluted with distilled water to form a 1 mg/mL solution. This solution was then mixed with iodine-KI reagent, and measured at 620 nm using an Evolution 201 UV-Visible Spectrophotometer (Thermo Scientific Inc., Waltham, USA). The amylose content was determined using a standard curve established by a mixed solution of amylose and amylopectin.

2.8 Scanning electron microscopy (SEM)

MERS samples were spread onto circular metal stubs covered with double-sided adhesive carbon tape and then sputter-coated with gold. Images of starch granules were obtained using an EM-30 Plus scanning electron microscope (SEM, COXEM, South Korea) under an accelerating voltage of 20 kV at 500× magnification.

2.9 Small-angle X-ray scattering (SAXS)

SAXS measurements were performed on a SAXSess small-angle X-ray scattering (SAXS) system (Anton-Paar, Austria) according to our previous methods (Zhang, Chen, Li, Li, & Zhang, 2015; Zhang, Chen, Zhao, & Li, 2013; Zhang, Li, Liu, Xie, & Chen, 2013). Samples were measured at 50 mA and 40 kV using a PW3830 X-ray generator (PANalytical) equipped with an X-ray source of Cu Kα radiation (λ = 0.1542 nm). Each sample with a moisture content of about 60% was prepared and equilibrated at room temperature for 24 h, before being placed into a paste cell and measured for 5 min under X-ray. The data, recorded in an image plate, were collected using the IP Reader software using a PerkinElmer Storage Phosphor System. All collected data were normalized,

and the background intensity and smeared intensity were subtracted by using SAXSquant 2D software and SAXSquant 3.0 software, respectively.

2.10 X-ray diffraction (XRD)

XRD analysis was performed using an Xpert PRO di□ractometer (PANalytical B.V., Netherlands), operated at 40 mA and 40 kV with an X-ray source of Cu-Kα radiation (λ = 0.15424 nm). The range of the diffraction angle (2θ) was from 5° to 40° with a scanning speed of 10°/min and a scanning step of 0.033°. The characteristic diffraction peaks of the A-type crystal are mainly 9.9°, 11.2°, 15°, 17°, 18°, and 23.5°, and those of the V-type crystal were mainly 7.4°, 13.1°, and 20.1° (Singh, Dartois, & Kaur, 2010).

The MDI Jade 6.0 software was used to compute the crystallinity between 4° and 30° 2θ, according to our previous studies (Xu, Tan, Chen, Li, & Xie, 2019). The integrated areas of all crystalline peaks halo on the X-ray diffractogram was the crystallization area (A_c), and the integrated areas of the amorphous halo on the X-ray diffractogram was the amorphous region (A_a). The equations used for calculating A-type or V-type crystallinity are: X_A (%) or X_V (%) = 100 × A_c/(A_c + A_a); and the total crystallinity is calculated using X_{Total} (%) = X_A (%) + X_V (%).

2.11 Fourier-transform infrared (FITR)

FTIR spectra with a range of 4000 to 400 cm^{-1} were obtained on a Tensor 37 spectrometer (Bruker, Germany) with a DTGS (deuterated triglycine sulfate) detector using an attenuated total reflectance accessory. For each spectrum, 64 scans with air as the background were obtained at a resolution of 4 cm^{-1}.

2.12 ^{13}C Cross-polarized magic angle spinning nuclear magnetic resonance (CP/MAS NMR) spectroscopy

Solid-state ^{13}C CP/MAS NMR analysis was performed on a Bruker AVANCE III HD 400 spectrometer (Bruker, Germany) equipped with a 4-mm broadband double-resonance MAS probe. Approximately 500 mg of the sample was placed into the spinner and inserted into the center of the magnetic field. The NMR spectrum with CP and MAS was recorded at 100.613 MHz at a temperature of 295 K. Over 6000 scans were accumulated for each spectrum with a recycle delay of 2 s (Mihhalevski et al., 2012; Tan, Flanagan, Halley, Whittaker, & Gidley, 2007).

2.13 Statistical analysis

The data were statistically analyzed using the SPSS 22.0 statistical package and presented as the mean ± standard deviation (SD). The differences between the groups were estimated using an analysis of variance (ANOVA), and $p < 0.05$ was considered to indicate a statistically significant difference between the two groups. Pearson correlation analysis was also conducted to determine the relationships between GG content, the structures and digestibility.

3 Results

3.1 *In vitro* digestibility

Table 1 shows the digestibility of NRS and MERS samples. Compared with those of NRS, the SDC and RC contents of MERS samples remarkably increased. The migration of water molecules to the interior of the starch granules driven by the thermomechanical energy during extrusion could destroy the hydrogen bonding between the starch molecules and induce the reorganization of starch

197 molecules to form a more thermodynamically stable structure, leading to a significantly RDC content
198 (Wang et al., 2018). The addition of GG apparently reduced the digestibility of MERS. With the
199 addition of GG, the RDC content of MERS samples was decreased by 26–41.8% and the RC content
200 was increased by 27.1–41.5% gradually. The effect of extrusion on the SDC content was less
201 significant, with an increase from 9.2% to 20.6%.

202

203 Table 1. RDC, SDC and RC contents and pGI of NRS and MERS samples*

Samples	RDC content (%)	SDC content (%)	RC content (%)	pGI
NRS	95.0±0.2^{e}	3.4±1.1^{a}	1.6±0.9^{a}	–
MERS/GG-0	75.2±0.6^{d}	10.3±0.6^{b}	14.5±0.5^{a}	82.3±1.5^{d}
MERS/GG-2.5%	49.2±1.0^{c}	9.2±0.9^{a}	41.6±1.2^{b}	64.3±2.2^{c}
MERS/GG-5%	42.8±0.7^{c}	11.2±0.5^{c}	46.0±0.2^{c}	63.2±0.9^{b}
MERS/GG-7.5%	33.2±1.5^{b}	16.4±1.4^{d}	50.4±1.7^{d}	63.0±1.3^{b}
MERS/GG-10%	23.4±1.1^{a}	20.6±0.2^{e}	56.0±0.9^{e}	61.8±1.2^{a}

204 * Mean value ± standard deviation of duplicate analysis is given. Values with di□erent letters within
205 the same column di□er significantly ($p < 0.05$).

206

207 **3.2 Predicted glycemic index (pGI)**

208 Table 1 also shows the pGI values of NRS and MERS samples. Specifically, the interaction with
209 GG significantly reduced the pGI of MERS. With increasing amounts of GG added, the pGI of
210 MERS decreased gradually. Along with the results about RC and SDC contents, it could be proposed
211 that the formation of SDC and RC reduced the pGI of MERS.

3.3 First-order kinetics analysis

Fig. 1 shows the digestibility curves and LoS plots for NRS and MERS samples. Table 2 shows the k and C_∞ values obtained from the LoS plots derived from the first-order kinetics of the digestion of MERS samples. In the first 1 h, MERS samples were digested rapidly and nearly reached a plateau at 80–120 min (Fig. 1A). In addition, for all MERS samples, the LoS plot exhibits a linear relationship with a constant k value, suggesting that the digestion of MERS was a single-phase process. The k value for MERS/GG-0 was significantly higher than that for MERS samples with GG (Table 2). C_∞ represents the theoretical percentage of starch digested at the end of the reaction. The addition of GG obviously reduced the C_∞ values for MERS samples. These results were consistent with the digestibility data as shown in Table 1.

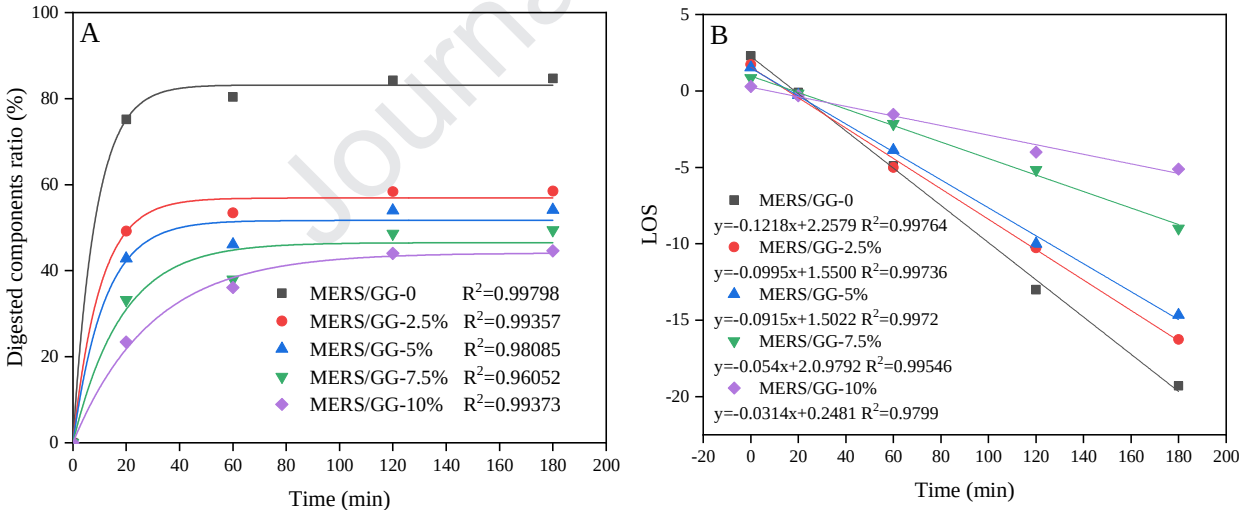

Fig. 1. Digestibility curves (A) and associated LoS plots (B) for MERS samples.

Table 2. Digestibility parameters obtained from the LoS plots for MERS samples*

Samples	k (min^{-1})	C_∞ (%)

MERS/GG-0	0.122±0.003^{d}	83.169±1.104^{c}
MERS/GG-2.5%	0.099±0.003^{c}	56.898±1.353^{b}
MERS/GG-5%	0.092±0.002^{c}	51.682±2.148^{b}
MERS/GG-7.5%	0.054±0.002^{b}	46.504±2.956^{a}
MERS/GG-10%	0.031±0.002^{a}	44.124±1.283^{a}

227 *Mean value ± standard deviation of duplicate analysis is given. Values with di□erent letters within
228 the same column di□er significantly ($p < 0.05$).

229

230 **3.4 Molecular mass distribution and amylose content**

231 The weight-average molecular mass (M_w), mean square radius of gyration, and molecular
232 mass distribution of NRS and MERS/GG-0 were investigated by GPC-MALS. The parameters of the
233 different samples are shown in Table 3. The M_w and R_g of NRS were 2.250×10^{7} g/mol and 112.9 nm,
234 respectively. After extrusion, the M_w of MERS/GG-0 decreased to 1.048×10^{7} g/mol. Along with that,
235 the R_g of MERS/GG-0 also decreased. These results show that the thermomechanical treatment could
236 break starch chains, reducing the molecular weight and the size of chain aggregates. Table 3 also
237 shows the cumulative weight fractions at different molecular mass distribution ranges for MERS
238 samples. For NRS, the fractions higher than 1×10^{7} g/mol accounted for 100%. After extrusion, the
239 molecular mass distribution of MERS/GG-0 moved towards lower values.

240

241 Table 3 GPC-MALS parameters of NRS and MERS/GG-0.

Samples	Amylose content	M_w (g/mol)	R_g	Molecular mass distribution (%)			
				<10^{6b}	1–5×10^{6b}	0.5–1×10^{7b}	>10^{7b}
NRS	22.90%	2.250×10^{7}	112.9 (0.5%)	0	0	0	100%

		(1%)[a]					
MERS/GG-0	25.30%	1.048×10^{7} (0.9%)	94.0 (0.5%)	0	23.6%	30.7%	45.8%

a. Fitting precision. b. g/mol.

Table 3 also shows the amylose contents of NRS and MERS/GG-0. Along with the molecular mass distribution results measured by GPC-MALS, it could be found that the thermomechanical treatment caused the breakage of α-1,4 glyosidic and α-1,6 glyosidic bonds, with increasing amylose content.

3.5 Granule microscopy

Fig. 2 shows the granule morphology of NRS and MERS samples. The granules of MERS presented irregular shapes and a rough surface, with pores on the surface. This indicates that the thermomechanical treatment significantly destroyed the granule structure of NRS. In comparison, the size of MERS became more homogeneous, ranging from 80 to 150 μm. MERS samples with GG were in the form of polygonal chunks with a smooth surface without apparent porosity, and the size of MERS with GG was approximately 120 μm. This indicates that the addition of GG significantly destroyed the granule morphology of MERS.

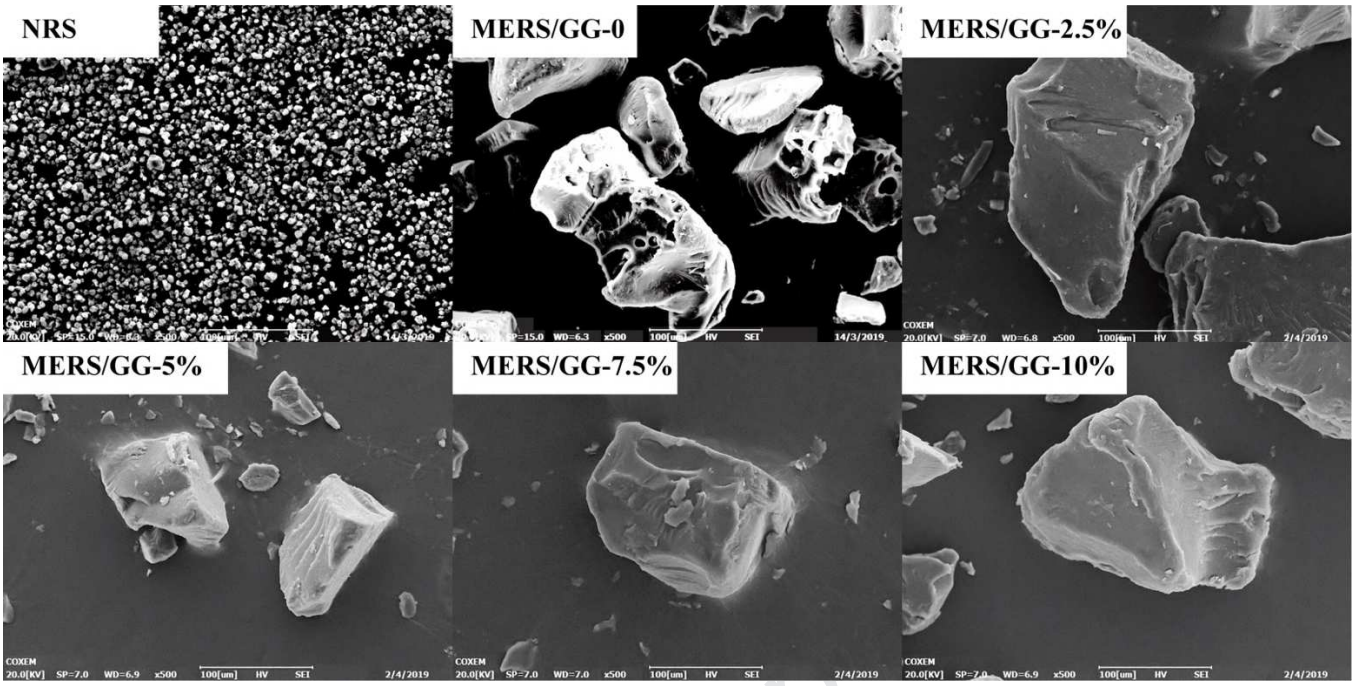

Fig. 2 SEM images of NRS and MERS samples (scale bar: 100 μm; magnification: ×500)

3.6 Fractal structure

Fig. 3 shows double-logarithmic SAXS curves for NRS and MERS samples. While NRS showed a characteristic scattering peak at q of 0.614 nm^{-1} representing its lamellar structure, this peak disappeared for all MERS samples either without or with GG, indicating the lamellar structure was completely destroyed by thermomechanical treatment. The α value (Table 4) was calculated by fitting the SAXS scattering signal to the power-law equation, $I(q) \sim q^{-\alpha}$, where I is the SAXS scattering intensity and α, obtained from the slope of the regression line of the double logarithmic SAXS curves, can be used to analyze the D characteristics of the surface/mass fractal structure. The scattering objects displayed a surface fractal structure with a fractal dimension $D_s = 6-\alpha$ in the case of $3 < \alpha < 4$, whereas a mass fractal structure was described with a fractal dimension $D_m = \alpha$ in the case of $1 < \alpha < 3$ (Cameron & Donald, 1993a, b). The fractal dimension of rice starch after extrusion

increased significantly. This suggests that the thermomechanical treatment caused the migration of water molecules to the interior of the starch granules, which destroyed the hydrogen bonding between starch chains and induced the reorganization of starch chains to form new aggregates. Compared with that of MERS/GG-0, the fractal dimension of MERS with GG was significantly larger. With increasing amounts of GG added, the fractal dimension of MERS and the density of nano-aggregates increased moderately.

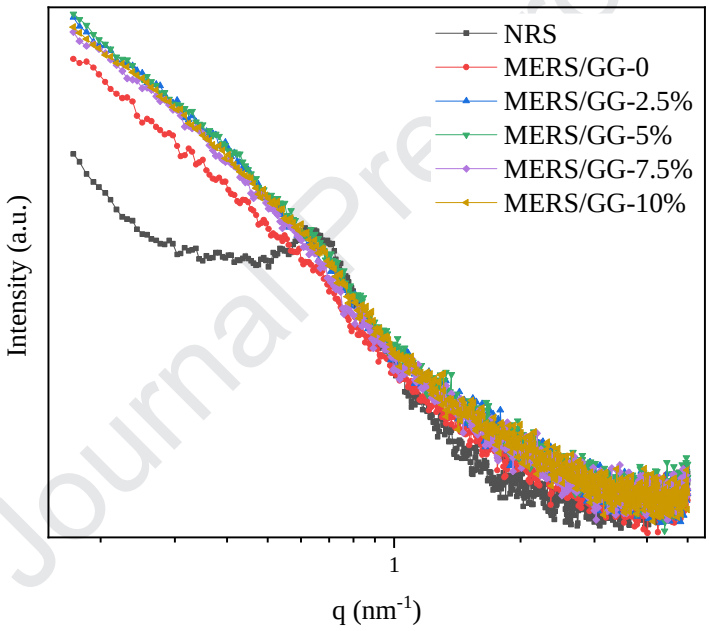

Fig. 3 Double-logarithmic SAXS patterns of NRS and MERS samples.

Table 4. α, total crystallinity (X_{Total}), A-type crystallinity (X_A), and V-type crystallinity (X_V) of NRS and MERS samples*

Samples	α	X_{Total} (%)	X_A (%)	X_V (%)
NRS	1.66±0.02^a	32.4±0.5^f	32.0±0.4^e	0.4±0.1^a
MERS/GG-0	2.10±0.02^b	17.8±0.3^a	16.0±0.1^a	1.8±0.2^b
MERS/GG-2.5%	2.27±0.01^c	19.7±0.3^b	16.5±0.2^b	3.2±0.1^c

MERS/GG-5%	2.28±0.02^{d}	21.5±0.2^{c}	17.6±0.1^{c}	3.9±0.1^{c}
MERS/GG-7.5%	2.31±0.03^{e}	22.5±0.3^{d}	18.3±0.2^{d}	4.2±0.1^{d}
MERS/GG-10%	2.33±0.01^{f}	23.3±0.4^{e}	18.7±0.2^{d}	4.6±0.2^{d}

283 *Mean value ± standard deviation of duplicate analysis was given. Values with di□erent letters
284 within the same column di□er significantly ($p < 0.05$).
285

286 **3.7 Crystalline structure**

287 Fig. 4 shows the XRD spectra of MERS samples. After extrusion, the rice starch maintained its
288 A-type crystal structure, but the intensity of characteristic diffraction peaks at 15°, 17°, 18° and 23.3°
289 (2θ) was significantly reduced, indicating reduced A-type crystallinity. The V-type crystalline
290 scattering peak increased significantly after extrusion. Regarding this, the thermomechanical
291 treatment may have caused the unwinding of double helices into single helices and the complexation
292 between amylose and the starch granule endogenous lipid (Wang et al., 2018). MERS/GG-0 shows
293 an A+V hybrid crystalline type. For MERS samples with GG, while the starch crystalline type
294 remained the same, the diffraction peak intensity increased. As shown in Table 4, the addition of GG
295 apparently increased the crystallinity of MERS, which was more so with a higher content of GG.
296

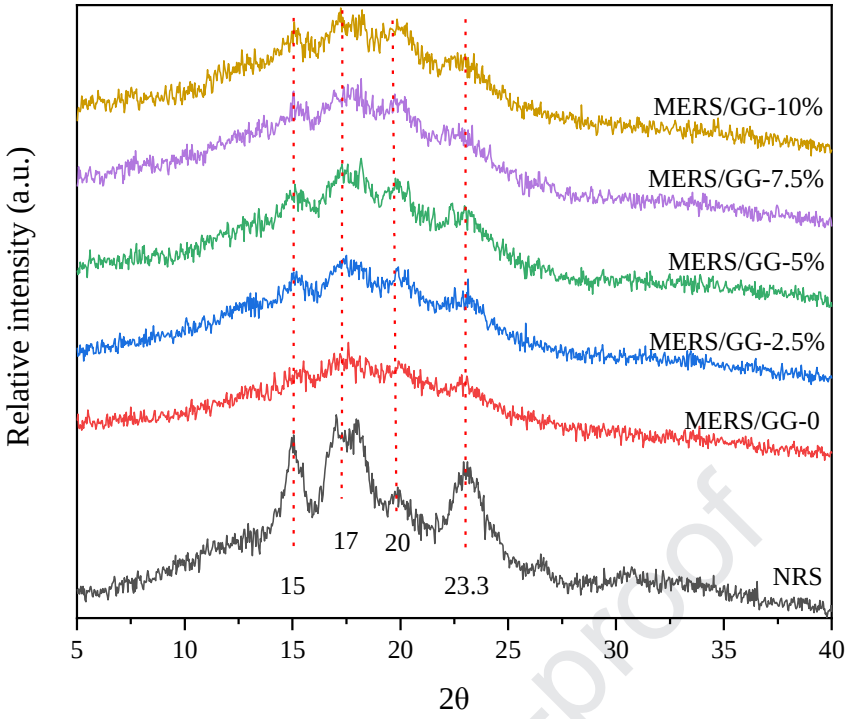

297

298 Fig. 4 X-ray diffraction patterns for NRS and MERS samples.

299

300 **3.8 FTIR analysis**

301 Fig. 5 shows the FTIR spectra for GG and MERS samples. The bands at 1047 cm^{-1}, 1081 cm^{-1}

302 and 1022 cm^{-1} can be attributed to the C─O stretching vibration of the anhydroglucose unit (AGU);

303 and additional strong signals at 3320 cm^{-1} and 2932 cm^{-1} could be assigned to O─H and C─H

304 stretching vibrations (Fang, Fowler, Tomkinson, & Hill, 2002; Zhou et al., 2014). The infrared

305 spectrum of GG was similar to that of MERS samples without or with GG. No new reflections were

306 detected for the complexation between rice starch and GG. With increasing amounts of GG added,

307 this absorption peak at around 3,300 cm^{-1} red-shifted gradually with increasing intensity, indicating

308 hydrogen-bonding interactions between GG and starch chains.

309

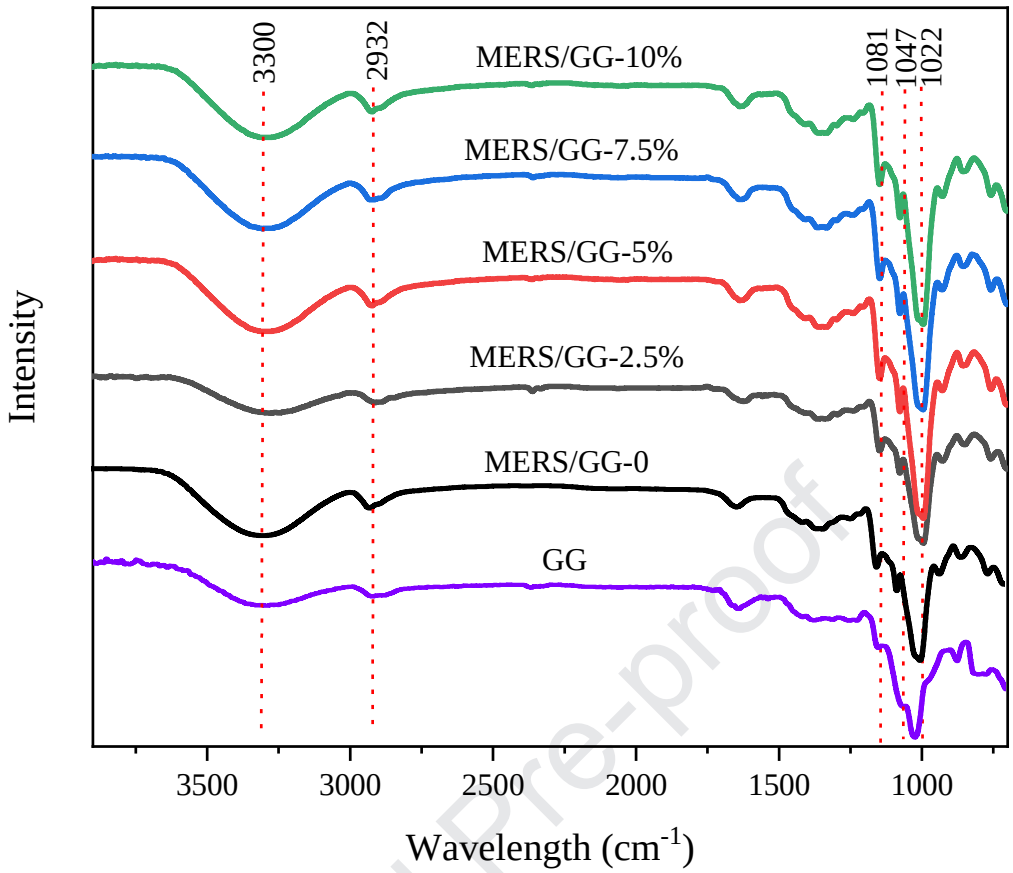

Fig. 5 FT-IR spectra for GG and MERS samples.

The complexation between GG and rice starch could change the starch molecular conformation and chain interactions. Fig. 6 shows the second-order derivative infrared spectra for MERS samples. The peak at 991 cm^{-1} represents the vibration absorption of C─O─H, which is related to hydrogen bonding associated with the C_6 hydroxyl group of the AGU of starch (Soest, Tournois, Wit, & Vliegenthart, 1995). Compared with MERS/GG-0, the addition of GG red-shifted the absorption peak of C─O─H at 991 cm^{-1}, and higher amounts of GG led to a greater shift. This result suggests that GG molecules could destroy the original hydrogen bonding in starch molecules by forming new hydrogen bonds with the starch AGU, which is in agreement with the infrared spectroscopy data in Fig. 5.

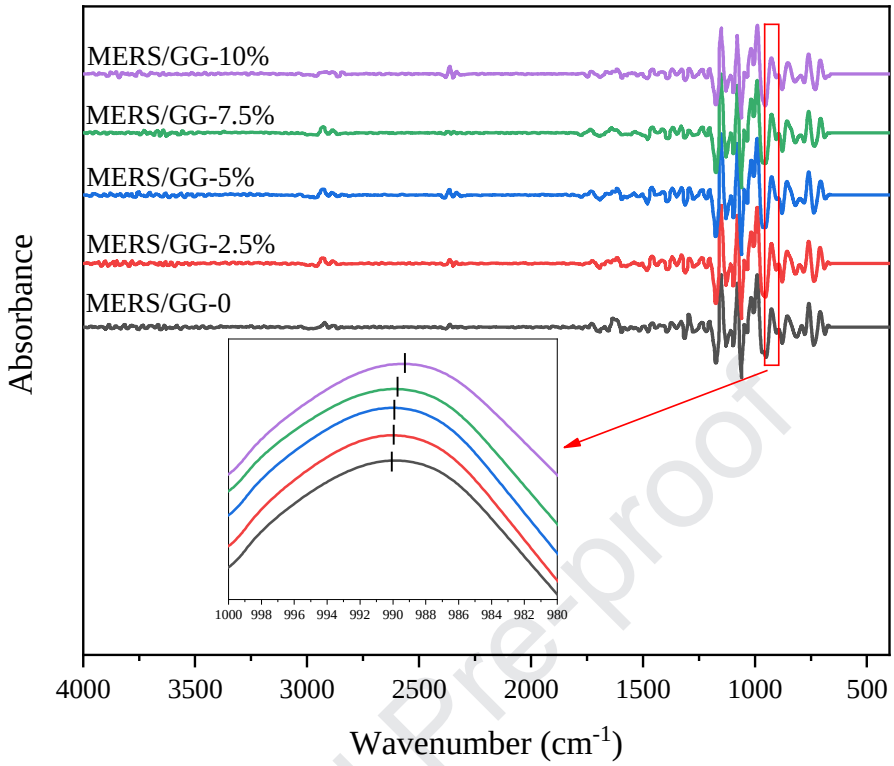

Fig. 6 Second-derivative infrared spectra for MERS samples.

A mechanistic analysis of the change in starch digestibility was performed by studying the change in the short-range ordered structure of starch. Fig. 7 shows an infrared deconvolution map for MERS samples, which could be used to calculate the degree of short-range ordering of the starch granule surface structure based on the ratio of intensity at 1,045/1,022 cm^{-1}. As shown in Table 5, during extrusion, the semi-crystalline structure was completely destroyed, and the degree of starch ordering was reduced; however, the hydro-thermo-mechanical treatment could lead to the reassembly of starch chains and thus a higher degree of aggregation (Wang, Li, Copeland, Niu, & Wang, 2015; Wang, Wang, Wang, & Wang, 2017). Complexation with GG improved the ordered structure of the starch granule surface, which was more apparent with higher amounts of GG added.

335

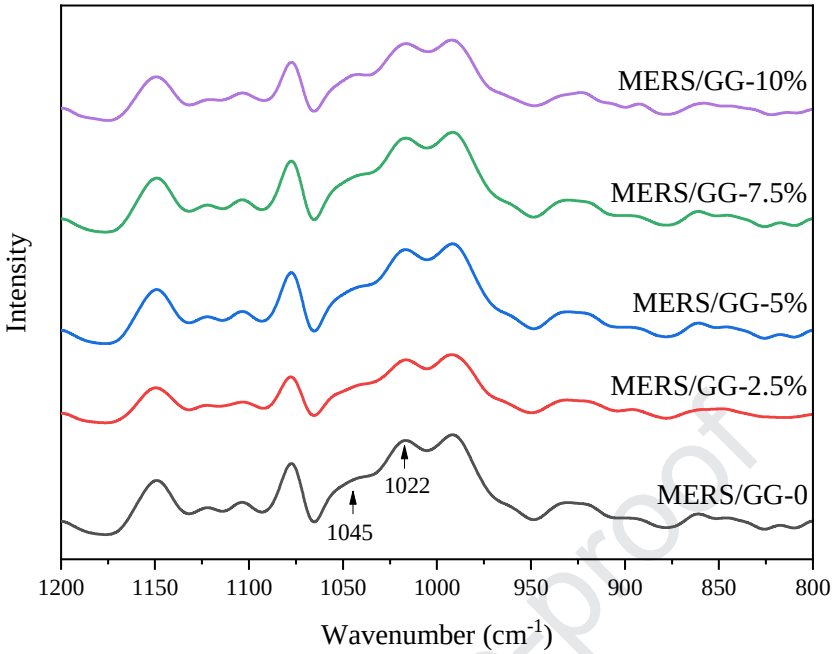

336

337 Fig. 7 Infrared deconvolution map for MERS samples.

338

339 Table 5. $R_{1045/1022}$ and proportions of amorphous starch and helical structures of MERS samples*

Samples	$R_{1045/1022}$	Amorphous starch	Single helix	Double helix
MERS/GG-0	0.815±0.002^{a}	79.2±0.5^{e}	2.5±0.3^{a}	18.3±0.8^{a}
MERS/GG-2.5%	0.833±0.014^{b}	77.7±0.1^{d}	3.1±0.3^{b}	19.2±0.2^{b}
MERS/GG-5%	0.837±0.002^{c}	74.4±0.1^{c}	5.9±0.0^{c}	19.7±0.1^{b}
MERS/GG-7.5%	0.845±0.013^{d}	72.6±0.5^{b}	6.8±0.3^{d}	20.6±0.8^{c}
MERS/GG-10%	0.870±0.006^{e}	70.4±0.1^{a}	7.9±0.0^{e}	21.7±0.0^{d}

340 *Mean value ± standard deviation of duplicate analysis is given. Values with di□erent letters within

341 the same column di□er significantly ($p < 0.05$).

342

3.9 ^{13}C CP/MAS NMR Analysis

The change in the helical structure of MERS samples was studied by ^{13}C CP/MAS NMR and the results are shown in Fig. 8 and Table 5. For MERS samples with GG, the C_1 peak was located between 96 and 106 ppm, the C_4 peak between 80 and 85 ppm, the $C_{2,3,5}$ peak between 68 and 78 ppm, and the C_6 peak between 58 and 65 ppm. Peaks at 99–102 ppm in C_1 region indicate V-type single helices (eight glucose cycles per turn), and 103.2 ppm is also related to the amorphous starch content associated with the junction points of amylopectin double helices. In addition, the peaks centered on 101.5, 100.5, and 99.4 ppm in the C_1 region are characteristic of the double-helical structure of A-type starch (Gidley & Bociek, 2002; Morrison, Tester, Gidley, & Karkalas, 1993). The ratio between the area of these characteristic peaks and the area of the C_1 peak can be used to calculate the proportions of single/double helices and amorphous structure (Fan et al., 2013). The thermomechanical treatment can easily induce the breakage of starch α-1,6 glyosidic bonds, further increasing the amylose content and promoting the formation of single helices (Liu et al., 2017). Increasing amounts of GG led to higher amounts of single helices, a lower proportion of double helices, and less amorphous content.

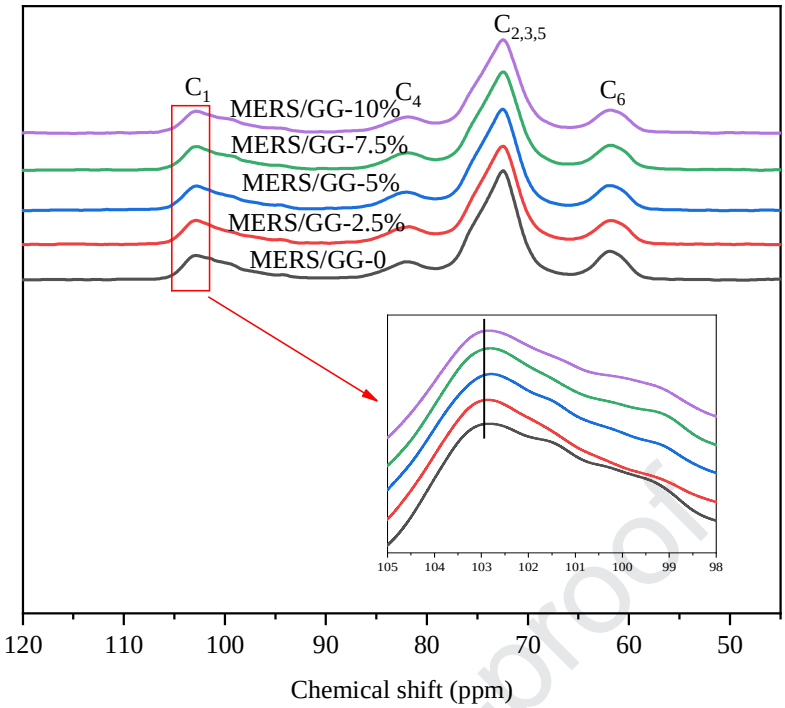

Fig. 8 ^{13}C CP/MAS NMR spectra for MERS samples

4 Discussion

The thermomechanical treatment by extrusion facilitates the interaction of starch chains with water, causes changes in the starch multiscale structures (granule morphology, semi-crystalline structure, crystallites, and helical structures) and the structural ordering, and leads to the formation of new starch aggregates. These structural changes vary the digestibility and the blood glucose response level of rice starch.

GG can be incorporated into starch-based food products through forming hydrogen bonding, van der Waals forces, and other non-covalent forces with starch chains. These interactions induce the rearrangement of starch chains to form more-ordered aggregates, which are more resistant to amylase (Zheng et al., 2019). Besides, the aqueous solution formed by GG has a high viscosity,

372 which inhibits the migration of amylase in solution and thus restricts the access of amylase to starch
373 chains (Sasaki & Kohyama, 2012). Moreover, Slaughter et al. (Slaughter, Ellis, Jackson, &
374 Butterworth, 2002) have suggested that some parts of an enzyme molecule may have a certain
375 affinity with GG, making GG a non-competitive inhibitor for the α-amylase-catalyzed hydrolysis of
376 starch molecules.

377 Fig. 9 shows a schematic representation of the non-covalent interaction of GG with rice starch
378 during extrusion and the associated changes in the multi-scale structures and digestibility of rice
379 starch. The thermomechanical treatment could facilitate hydrogen-bonding interactions between GG
380 and starch chains and the formation of new aggregates (i.e., single- or double-helices), which
381 effectively shielded the action sites on starch chains for amylase and thus reduced the hydrolysis by
382 amylase.

383 At a low content of GG addition (up to 10%), the complexation between GG and starch chains
384 led to a significantly higher RC content (Table 1). Regarding this, GG increased the ordering of the
385 aggregated structure (Fig. 3 and Table 4), the contents of single- and double-helices (Fig. 8 and Table
386 5), X_A and X_V (Fig. 4 and Table 4), thereby improving the digestion resistance.

387

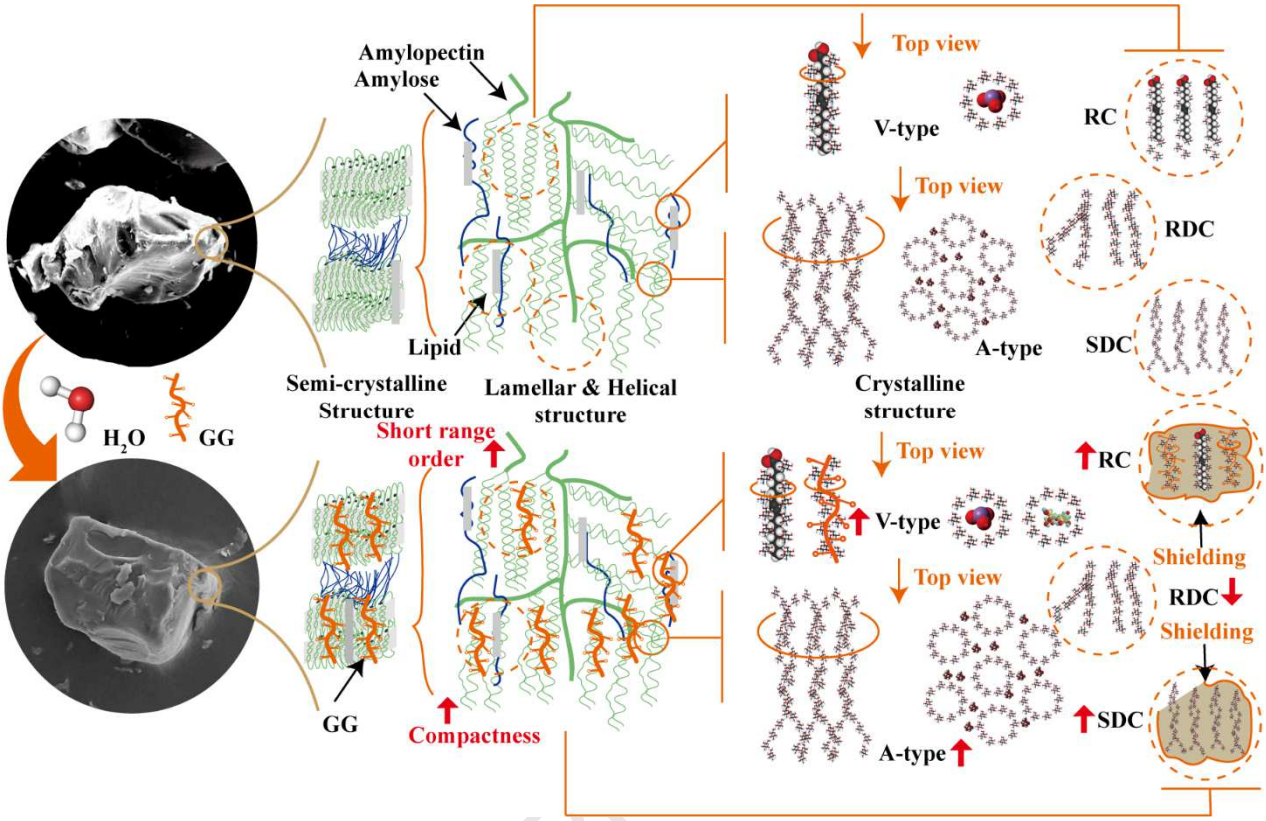

388

389 Fig. 9 Schematic representation for the changes of multi-scale structure and digestibility of MERS

390 samples.

391

392 As the GG content increases, GG begins to adhere and wrap the starch granule fragments and

393 the structure of the rice starch-GG complex becomes denser (Zhang, Gu, Hong, & Cai, 2012). In

394 other words, with more GG added, GG may provide a spatial resistance (Bordoloi et al., 2012;

395 Dartois, Singh, Kaur, & Singh, 2010). Increasing the amount of GG enhances the interaction

396 between GG and starch chains and promotes the formation of an ordered, complexed structure

397 (Zheng et al., 2019). While the ordered structure formed by starch chains highly depends on strong

398 hydrogen bonding interactions and chain arrangements, there are also many weak hydrogen bonds

399 between starch chains. The co-existence of these hydrogen bonds with different strengths results in a

400 wider frequency range of the characteristic peak of hydroxyls (Bemiller & Huber, 2015). As amylose

readily forms complexes with organic molecules such as GG especially during thermomechanical processing (Chaisawang & Suphantharika, 2005), the complexation can lead to increased V-type crystallinity.

In ^{13}C CP/MAS NMR spectra, the position of C_1 is related to the helical structure, as the spiral arrangement of glucose molecules in V_6, V_7, and V_8 structures is different. In other words, as the bonding position of hydrogen bonds is different, the chemical displacement position of the C_1 peak for the three types of helical structure varies. The C_1 chemical displacement signals of the V_6, V_7, and V_8 helical structures are 102.2–102.7 ppm, 103.3–103.4 ppm, and 103.9–104.3 ppm, respectively (Bail, Rondeau, & Buleon, 2005). A higher chemical displacement value of general C_1 indicates a greater amount of helical structure in starch (Tian et al., 2018). The chemical displacement of C_1 for MERS with GG was close to the V_6 value, indicating that the single-helical structure in the complex was of two main types, namely V_6 and V_7.

Table 6 shows the results of Pearson correlation analysis between the GG content and the structure and digestive properties of MERS with GG. There was a significant correlation between the RDC, SDC, and RC contents. The RDC content was significantly negatively correlated with the SDC content (−0.997, $p < 0.01$), RC content (−0.998, $p < 0.01$), α (−0.994, $p < 0.01$), X_{Total} (−0.959, $p < 0.05$), X_A (−0.955, $p < 0.05$), X_V (−0.962, $p < 0.05$), $R_{1047/1022}$ (−0.950, $p < 0.05$), single-helix content (−0.952, $p < 0.05$), and double-helix content (−0.997, $p < 0.01$), and was significantly positively correlated with amorphous starch content (0.975, $p < 0.05$). In addition, the RC content was significantly positively correlated with α (0.985, $p < 0.05$), X_{Total} (0.970, $p < 0.05$), X_A (0.964, $p < 0.05$), X_V (0.976, $p < 0.05$), $R_{1047/1022}$ (0.987, $p < 0.05$), single-helix content (0.950, $p < 0.05$), and

422 double-helix content (0.994, $p < 0.01$), and was significantly negatively correlated with amorphous
423 starch content (−0.986, $p < 0.05$). The addition of GG was significantly positively correlated with α
424 (0.984, $p < 0.05$), X_{Total} (0.981, $p < 0.05$), X_A (0.978, $p < 0.05$), X_V (0.983, $p < 0.05$), single-helix
425 content (0.962, $p < 0.05$), and double-helix content (0.987, $p < 0.05$). In addition, GG content was
426 strongly negatively correlated with pGI (−0.970, $p < 0.05$), which means the level of postprandial
427 blood glucose response to MERS could be reduced by increasing the amount of GG added. RDC and
428 pGI were positively correlated with each other (0.960, $p < 0.05$), while the RDC and RC contents
429 were negatively correlated (−0.998, $p < 0.01$). This indicates that GG reduced the RDC content and
430 increased the RC content by changing the RC content, X_V, X_A, and the amounts of single- and
431 double-helices.

432

433 Table 6. Pearson correlation coefficients of GG content with starch structures and digestibility

	GG content	RDC content	SDC content	RC content
GG content	1	–	–	–
RDC content	−0.996**	1	–	–
SDC content	0.987*	−0.997**	1	–
RC content	0.998**	−0.998**	0.989*	1
α	0.984*	−0.994**	0.999**	0.985*
X_{Total}	0.981*	−0.959*	0.940	0.970*
X_A	0.978*	−0.955*	0.938	0.964*
X_V	0.983*	−0.962*	0.941	0.976*
$R_{1047/1022}$	0.925	−0.950*	0.948	0.987*
Amorphous starch content	−0.992**	0.975*	−0.957*	−0.986*
Single helix content	0.962*	−0.952*	0.906	0.950*

Double helix content	0.987*	−0.997**	0.996	0.994**
pGI	−0.970*	0.960*	−0.936	−0.976*

Mean value ± standard deviation of duplicate analysis is given; $^{*}p < 0.05$, $^{**}p < 0.01$.

5 Conclusion

For MERS, the addition of GG significantly increased the RC content and reduced pGI. Moreover, MERS with GG showed increases in the degrees of the ordering of nano-aggregates and the granule surface structure, higher crystallinity (X_{Total}, X_A, and X_V), and greater amounts of single- and double- helices. Pearson correlation analysis shows that X_{Total}, X_A, X_V, and single- and double-helix contents were correlated with the SDC and RC contents. Thus, this study demonstrates that the starch structure and digestibility could be well regulated by the addition of GG combined with thermomechanical treatment.

Acknowledgements

The authors thank for the financial support provided by the National Natural Science Foundation of China (NSFC)–Guangdong Joint Fund under a Key Project (No. U1501214), the National Natural Science Foundation of China (NSFC) under a General Project (No. 31871751), the Guangzhou Science and Technology Program under a Key Project (No.201804020036) and the Guangdong Provincial Government under a YangFan Innovative and Entrepreneurial Research Team Project (2014YT02S029). F. Xie acknowledges the support from the European Union's Horizon 2020 research and innovation programme under the Marie Skłodowska-Curie grant agreement No. 798225.

Conflicts of interest

There are no conflicts of interest to declare.

References

Bail, P. Y., Rondeau, C., & Buleon, A. (2005). Structural investigation of amylose complexes with small ligands: helical conformation, crystalline structure and thermostability. *International Journal of Biological Macromolecules, 35*(1), 1-7. https://doi.org/10.1016/j.ijbiomac.2004.09.001

Bemiller, J. N., & Huber, K. C. (2015). Physical Modification of Food Starch Functionalities. *Annual Review of Food Science and Technology, 6*(1), 19-69. https://doi.org/10.1146/annurev-food-022814-015552

Bordoloi, A., Singh, J., & Kaur, L. (2012). In vitro digestibility of starch in cooked potatoes as affected by guar gum: Microstructural and rheological characteristics. *Food Chemistry, 133*(4), 1206-1213. https://doi.org/10.1016/j.foodchem.2012.01.063

Butt, M. S., Shahzadi, N., Sharif, M. K., & Nasir, M. (2007). Guar Gum: A Miracle Therapy for Hypercholesterolemia, Hyperglycemia and Obesity. *Critical Reviews in Food Science and Nutrition, 47*(4), 389-396. https://doi.org/10.1080/10408390600846267

Butterworth, P. J., Frederick, J. W., Terri, G., Hamung, P., & Peter, R. E. (2012). Analysis of starch amylolysis using plots for first-order kinetics. *Carbohydrate Polymers, 87*(3), 2189-2197. http://dx.doi.org/10.1016/j.carbpol.2011.10.048

Cameron, R. E., & Donald, A. M. (1993a). A small-angle X-ray scattering study of the absorption of water into the starch granule. *Carbohydrate Research, 244*(2), 225-236. https://doi.org/10.1016/0008-6215(83)85003-4

Cameron, R. E., & Donald, A. M. (1993b). A small□angle x□ray scattering study of starch gelatinization in excess and limiting water. *Journal of Polymer Science Part B Polymer Physics, 31*(9), 1197-1203. https://doi.org/10.1016/0008-6215(83)85003-4

Chaisawang, M., & Suphantharika, M. (2005). Effects of guar gum and xanthan gum additions on physical and rheological properties of cationic tapioca starch. *Carbohydrate Polymers, 61*(3), 288-295. https://doi.org/10.1016/j.carbpol.2005.04.002

Chung, H. J., Liu, Q., & Lim, S. T. (2007). Texture and in vitro digestibility of white rice cooked with hydrocolloids. *Cereal Chemistry, 84*(3), 246-249. https://doi.org/10.1094/CCHEM-84-3-0246

Crawford, M. A., Broadhurst, C. L., Cunnane, S., Marsh, D. E., Schmidt, W. F., Brand, A., & Ghebremeskel, K. (2014). Nutritional armor in evolution: docosahexaenoic acid as a determinant of neural, evolution and hominid brain development. *Military Medicine, 179*(11), 61-75. https://doi.org/10.7205/MILMED-D-14-00246

Dartois, A., Singh, J., Kaur, L., & Singh, H. (2010). Influence of Guar Gum on the In Vitro Starch Digestibility—Rheological and Microstructural Characteristics. *Food Biophysics, 5*(3), 149-160. https://doi.org/10.1007/s11483-010-9155-2

Dhital, S., Warren, F. J., Butterworth, P. J., Ellis, P. R., & Gidley, M. J. (2017). Mechanisms of Starch Digestion by α-amylase–structural Basis for Kinetic Properties. *Critical Reviews in Food Science and Nutrition, 57*(5), 875-892. http://dx.doi.org/10.1080/10408398.2014.922043

Englyst, H. N., & Cummings, J. H. (1985). Digestion of the polysaccharides of some cereal foods in the human small intestine. *The American Journal of Clinical Nutrition, 42*(5), 778-787. https://doi.org/10.1016/S0271-5317(85)80148-2

Fan, D., Ma, W., Wang, L., Huang, J., Zhang, F., Zhao, J., Zhang, H., & Chen, W. (2013). Determining the effects of microwave heating on the ordered structures of rice starch by NMR. *Carbohydrate Polymers, 92*(2), 1395-1401. https://doi.org/10.1016/j.carbpol.2012.09.072

Fan, J., Yu, D., Han, B., Kou, M., Niu, F., Gu, Z., & Pan, W. (2018). Effects of screw extrusion on digestibility and glycemic index of potato starch. *Journal of Food Safety and Quality, 9*(14), 207-212. https://doi.org/CNKI:SUN:SPAJ.0.2018-14-043

Fang, C. G., Li, Q., & Liu, S. J. (2016). Promoting the sustained and healthy development of the food safety risk monitoring work of Jilin provincial center for disease control and prevention

with concept of science and technology innovation. *Journal of Food Safety and Quality, 7*(1), 3-7. https://doi.org/CNKI:SUN:SPAJ.0.2016-01-002

Fang, J. M., Fowler, P. A., Tomkinson, J., & Hill, C. A. S. (2002). The preparation and characterisation of a series of chemically modified potato starches. *Carbohydrate Polymers, 47*(3), 245-252. https://doi.org/10.1016/s0144-8617(01)00187-4

Gidley, M. J., & Bociek, S. M. (2002). Carbon-13 CP/MAS NMR studies of amylose inclusion complexes, cyclodextrins, and the amorphous phase of starch granules: relationships between glycosidic linkage conformation and solid-state carbon-13 chemical shifts. *Journal of the American Chemical Society, 110*(12), 3820-3829. https://doi.org/10.1021/ja00220a016

Gomez, M. H., & Aguilera, J. M. (2010). Changes in the Starch Fraction During Extrusion□cooking of Corn. *Journal of Food Science, 48*(2), 378-381. https://doi.org/10.1111/j.1365-2621.1983.tb10747.x

Goñi, I., Garciaalonso, A., & Sauracalixto, F. (1997). A starch hydrolysis procedure to estimate glycemic index. *Nutrition Research, 17*(3), 427-437. https://doi.org/10.1016/s0271-5317(97)00010-9

Guerrant, N. B., Dutcher, R. A., & Brown, R. A. (1937). Further studies concerning the formation of the B-vitamins in the digestive tract of the rat. *The Journal of Nutrition, 13*(3), 305-315. https://doi.org/10.1093/jn/13.3.305

Jang, H. L., Bae, I. Y., & Lee, H. G. (2015). In vitro starch digestibility of noodles with various cereal flours and hydrocolloids. *LWT-Food Science and Technology, 63*(1), 122-128. https://doi.org/10.1016/j.lwt.2015.03.029

Jenkins, D. J., Wolever, T. M., Taylor, R. H., Barker, H., Fielden, H., Baldwin, J. M., Bowling, A. C., Newman, H. C., Jenkins, A. L., & Goff, D. V. (1981). Glycemic index of foods: a physiological basis for carbohydrate exchange. *The American Journal of Clinical Nutrition, 34*(3), 362-366. https://doi.org/10.1093/ajcn/34.3.362

Lai, L. S., & Kokini, J. L. (1991). Physicochemical Changes and Rheological Properties of Starch during Extrusion (A Review). *Biotechnology Progress, 7*(3), 251-266. https://doi.org/10.1021/bp00009a009

Lim, Y. M., Hoobin, P., Ying, D., Burgar, I., Gooley, P. R., & Augustin, M. A. (2015). Physical characterisation of high amylose maize starch and acylated high amylose maize starches. *Carbohydrate Polymers, 117*, 279-285. https://doi.org/10.1016/j.carbpol.2014.09.068

Liu, X., Xiao, X., Liu, P., Yu, L., Li, M., Zhou, S., & Xie, F. (2017). Shear degradation of corn starches with different amylose contents. *Food Hydrocolloids, 66*, 199-205. https://doi.org/10.1016/j.foodhyd.2016.11.023

Liu, Y., Chen, L., Xu, H., Liang, Y., & Zheng, B. (2019). Understanding the digestibility of rice starch-gallic acid complexes formed by high pressure homogenization. *International Journal of Biological Macromolecules, 134*, 856-863. https://doi.org/10.1016/j.ijbiomac.2019.05.083

Mihhalevski, A., Heinmaa, I., Traksmaa, R., Pehk, T., Mere, A., & Paalme, T. (2012). Structural changes of starch during baking and staling of rye bread. *Journal of Agricultural and Food Chemistry, 60*(34), 8492-8500. https://doi.org/10.1021/jf3021877

Miller, J. B., Pang, E., & Bramall, L. (1992). Rice: a high or low glycemic index food? *The American Journal of Clinical Nutrition, 56*(6), 1034-1036. https://doi.org/10.1093/ajcn/56.6.1034

Morrison, W. R., Tester, R. F., Gidley, M. J., & Karkalas, J. (1993). Resistance to acid hydrolysis of lipid-complexed amylose and lipid-free amylose in lintnerised waxy and non-waxy barley starches. *Carbohydrate Research, 245*(2), 289-302. https://doi.org/10.1016/0008-6215(93)80078-S

Mudgil, D., Barak, S., & Khatkar, B. S. (2014). Guar gum: processing, properties and food applications-a review. *Journal of Food Science and Technology, 51*(3), 409-418. https://doi.org/10.1007/s13197-011-0522-x

Roberts, S. B. (2000). High-glycemic index foods, hunger, and obesity: is there a connection? *Nutrition Reviews, 58*(6), 163-169. https://doi.org/10.1111/j.1753-4887.2000.tb01855.x

Sasaki, T., & Kohyama, K. (2012). Influence of non-starch polysaccharides on the in vitro digestibility and viscosity of starch suspensions. *Food Chemistry, 133*(4), 1420-1426. https://doi.org/10.1016/j.foodchem.2012.02.029

562 Shahzadi, N., Butt, M. S., Sharif, M. K., & Nasir, M. (2007). Effect of guar gum on the serum lipid
563 profile of Sprague Dawley rats. *LWT-Food Science and Technology, 40*(7), 1198-1205.
564 https://doi.org/10.1016/j.lwt.2006.08.007
565 Singh, J., Dartois, A., & Kaur, L. (2010). Starch digestibility in food matrix: a review. *Trends in*
566 *Food Science and Technology, 21*(4), 168-180. https://doi.org/10.1016/j.tifs.2009.12.001
567 Slaughter, S. L., Ellis, P. R., Jackson, E. C., & Butterworth, P. J. (2002). The effect of guar
568 galactomannan and water availability during hydrothermal processing on the hydrolysis of
569 starch catalysed by pancreatic α-amylase. *Biochimica et Biophysica Acta 1571*(1), 55-63.
570 https://doi.org/10.1016/S0304-4165(02)00209-X
571 Soest, J. J. G. V., Tournois, H., Wit, D. D., & Vliegenthart, J. F. G. (1995). Short-range structure in
572 (partially) crystalline potato starch determined with attenuated total reflectance
573 Fourier-transform IR spectroscopy. *Carbohydrate Research, 279*(95), 201-214.
574 https://doi.org/10.1016/0008-6215(95)00270-7
575 Tan, I., Flanagan, B. M., Halley, P. J., Whittaker, A. K., & Gidley, M. J. (2007). A Method for
576 Estimating the Nature and Relative Proportions of Amorphous, Single, and Double-Helical
577 Components in Starch Granules by 13C CP/MAS NMR. *Biomacromolecules, 8*(3), 885-891.
578 https://doi.org/10.1021/bm060988a
579 Thompson, S. V., Winham, D. M., & Hutchins, A. M. (2012). Bean and rice meals reduce
580 postprandial glycemic response in adults with type 2 diabetes: a cross-over study. *Nutrition*
581 *Journal, 11*(1), 23-30. https://doi.org/10.1186/1475-2891-11-23
582 Tian, J., Ogawa, Y., Shi, J., Chen, S., Zhang, H., Liu, D., & Ye, X. (2018). The microstructure of
583 starchy food modulates its digestibility. *Critical Reviews in Food Science and Nutrition, 5*,
584 1-12. https://doi.org/10.1080/10408398.2018.1484341
585 Wang, H., Liu, Y., Chen, L., Li, X., Wang, J., & Xie, F. (2018). Insights into the multi-scale structure
586 and digestibility of heat-moisture treated rice starch. *Food Chemistry, 242*, 323-329.
587 Wang, H., Wang, Z., Li, X., Chen, L., & Zhang, B. (2017). Multi-scale structure, pasting and
588 digestibility of heat moisture treated red adzuki bean starch. *International Journal of*
589 *Biological Macromolecules, 102*, 162-169. https://doi.org/10.1016/j.ijbiomac.2017.03.144

590 Wang, S., Li, C., Copeland, L., Niu, Q., & Wang, S. (2015). Starch retrogradation: A comprehensive
591 review. *Comprehensive Reviews in Food Science and Food Safety, 14*(5), 568-585.
592 https://doi.org/10.1111/1541-4337.12143
593 Wang, S., Wang, J., Wang, S., & Wang, S. (2017). Annealing improves paste viscosity and stability
594 of starch. *Food Hydrocolloids, 62*, 203-211. https://doi.org/10.1016/j.foodhyd.2016.08.006
595 Xu, J., Kuang, Q., Wang, K., Zhou, S., & Wang, S. (2017). Insights into molecular structure and
596 digestion rate of oat starch. *Food Chemistry, 220*, 25-30.
597 http://dx.doi.org/10.1016/j.foodchem.2016.09.191
598 Xu, J., Tan, X., Chen, L., Li, X., & Xie, F. (2019). Starch/microcrystalline cellulose hybrid gels as
599 gastric-floating drug delivery systems. *Carbohydrate Polymers, 215*, 151-159.
600 https://doi.org/10.1016/j.carbpol.2019.03.078
601 Ye, J., Hu, X., Luo, S., Wei, L., & Liu, C. (2017). Properties of Starch after Extrusion: A Review.
602 *Starch □ Stärke*, *70*(11), 1700110-1700118. https://doi.org/10.1002/star.201700110
603 Zhang, B., Chen, L., Li, X., Li, L., & Zhang, H. (2015). Understanding the multi-scale structure and
604 functional properties of starch modulated by glow-plasma: A structure-functionality
605 relationship. *Food Hydrocolloid, 50*, 228-236. https://doi.org/10.1016/j.foodhyd.2015.05.002
606 Zhang, B., Chen, L., Zhao, Y., & Li, X. (2013). Structure and enzymatic resistivity of debranched
607 high temperature-pressure treated high-amylose corn starch. *Journal of Cereal Science, 57*(3),
608 348-355. https://doi.org/10.1016/j.jcs.2012.12.006
609 Zhang, B., Li, X., Liu, J., Xie, F., & Chen, L. (2013). Supramolecular structure of A- and B-type
610 granules of wheat starch. *Food Hydrocolloid, 31*(1), 68-73.
611 https://doi.org/10.1016/j.foodhyd.2012.10.006
612 Zhang, Y. Y., Gu, Z. B., Hong, Y., & Cai, X. R. (2012). Pasting and Rheological Properties of Starch
613 and Guar Gum Mixed Systems. *Food Science and Biotechnology, 31*(08), 820-825.
614 https://doi.org/10.3969/j.issn.1673-1689.2012.08.005
615 Zheng, M., You, Q., Lin, Y., Lan, F., Luo, M., Zeng, H., Zheng, B., & Zhang, Y. (2019). Effect of
616 guar gum on the physicochemical properties and in vitro digestibility of lotus seed starch.
617 *Food Chemistry, 272*, 286-291. https://doi.org/10.1016/j.foodchem.2018.08.029

618 Zhou, Z. K., Hua, Z. T., Yang, Y., Zheng, P. Y., Zhang, Y., & Chen, X. S. (2014). Molecular
619 Characteristics of New Wheat Starch and Its Digestion Behaviours. *Journal of Integrative*
620 *Agriculture, 13*(5), 1146-1153. https://doi.org/10.1016/S2095-3119(13)60621-8
621

Highlights

- ✓ Micro-extruded rice starch (MERS) was prepared with guar gum (GG)
- ✓ GG addition enhanced slowly-digestible (SDC) and resistant (RC) components in MERS
- ✓ MERS with GG presented reduced digestion rate and predicted glycemic index (pGI)
- ✓ Crystallinity and helical structures contributed to SDC and RC in MERS with GG

– Declaration of Interest –

Improving the *in vitro* digestibility of rice starch by thermomechanically assisted complexation with guar gum

Hai He[a], Chengdeng Chi[a], Fengwei Xie[b, c, *], Xiaoxi Li[a], Yi Liang[d], Ling Chen[a, *]

[a] Ministry of Education Engineering Research Center of Starch & Protein Processing, Guangdong Province Key Laboratory for Green Processing of Natural Products and Product Safety, School of Food Science and Engineering, South China University of Technology, Guangzhou, Guangdong, 510640, China.

[b] International Institute for Nanocomposites Manufacturing (IINM), WMG, University of Warwick, Coventry CV4 7AL, United Kingdom.

[c] School of Chemical Engineering, The University of Queensland, Brisbane, Qld 4072, Australia.

[d] Guangdong Zhongqing Font Biochemical Science and Technology Co., Ltd., Maoming, Guangdong 525427, China.

The authors declare that there is no conflict of interest regarding the publication of this article.